Numerical Methods for Stochastic Differential Equations
Modelling the Stock Price

Kelsey Bozic, Joost Fitton, STOCK5

January 31, 2025

1 Problem Description

We consider the system of Itô SDEs for the stock price S_t, stochastic volatility σ_t, and long-term averaged volatility ξ_t:

$$dS_t = \mu S_t dt + \sigma_t S_t dw_1, \tag{1}$$
$$d\sigma_t = \alpha(\xi_t - \sigma_t)dt + p dw_2, \tag{2}$$
$$d\xi_t = \beta(\sigma_t - \xi_t)dt, \tag{3}$$

with the initial conditions:

$$S_0 = 50, \quad \sigma_0 = 0.20, \quad \xi_0 = 0.20, \quad \mu = 0.10.$$

For $\alpha = 0$ and $p = 0$, this reduces to the Black-Scholes model:

$$dS_t = \mu S_t dt + \sigma S_t dw. \tag{4}$$

2 Implementation

This section details the implementation of the Euler and Milstein schemes for solving the given SDEs numerically.

2.1 Euler-Maruyama Scheme

Our first step is to derive the Euler-Maruyama scheme, which we do according to the derivation on page 14 of the BS notes (eq.14):

$$\begin{aligned} X_{t+\Delta t} &= X_t + \int_t^{t+\Delta t} f(X_s, s)\, ds + \int_t^{t+\Delta t} g(X_s, s)\, dW_s \\ &\approx X_t + \int_t^{t+\Delta t} f(X_t, t)\, ds + \int_t^{t+\Delta t} g(X_t, t)\, dW_s \end{aligned}$$

$$= X_t + f(X_t, t)\Delta t + g(X_t, t)(W_{t+\Delta t} - W_t)$$

Applying this to our scheme we get the following:

$$S_{t+\Delta t}^{(\mathrm{Euler})} = S_t + \mu S_t \Delta t + \sigma_t S_t \Delta W_{1,t}, \tag{5}$$
$$\sigma_{t+\Delta t}^{(\mathrm{Euler})} = \sigma_t + \alpha(\xi_t - \sigma_t)\Delta t + p\sigma_t \Delta W_{2,t}, \tag{6}$$
$$\xi_{t+\Delta t}^{(\mathrm{Euler})} = \xi_t - \alpha(\sigma_t - \xi_t)\Delta t. \tag{7}$$

where $\Delta W_{i,t} = W_{i,t+\Delta t} - W_{i,t} \sim \mathrm{N}(0, \Delta t)$ for $i = 1, 2$

Next we derive the Milstein scheme.

2.2 Milstein Scheme

From page 36, we get the Milstein scheme for a single scalar stochastic differential equation, namely:

$$X_{t+\Delta t} = X_t + f(X_t, t)\Delta t + g(X_t, t)\Delta W_t + \frac{1}{2} g(X_t, t)\frac{\partial g}{\partial x}\left(\Delta W_t^2 - \Delta t\right).$$

However, in this case we are dealing with both multiple SDE's and multiple noise inputs, and therefore will use (3.4) from p.346 of the book,

The system has $d = 3$ state variables: (S, σ, ξ) and is driven by $m = 2$ independent Wiener processes.

The general multi-dimensional Milstein scheme from equation (3.4) is:

$$Y_{n+1}^k = Y_n^k + a^k \Delta t + \sum_{j=1}^{m} b^{k,j} \Delta W^j + \sum_{j_1, j_2 = 1}^{m} L^{j_1} b^{k, j_2} J_{(j_1, j_2)}.$$

where:

- a^k are the drift terms.
- $b^{k,j}$ are the diffusion coefficients.
- L^{j_1} is the Lie derivative:

$$L^{j_1} = \sum_{i=1}^{d} b^{i, j_1} \frac{\partial}{\partial Y^i}.$$

- $J_{(j_1, j_2)}$ are the iterated stochastic integrals:

$$J_{(j_1, j_2)} = \int_{t_n}^{t_{n+1}} \int_{t_n}^{s} \mathrm{d}w_{j_1}(u) \mathrm{d}w_{j_2}(s).$$

For independent Brownian motions, these iterated integrals can be approximated as:

$$J_{(j,j)} \approx \frac{1}{2}\left[(\Delta W_j)^2 - \Delta t\right], \quad J_{(j_1,j_2)} \approx \Delta W_{j_1} \Delta W_{j_2}, \quad j_1 \neq j_2.$$

Discretizing for S_t
- Drift term:

$$a^1 = \mu S.$$

- Diffusion terms:

$$b^{1,1} = \sigma S, \quad b^{1,2} = 0.$$

Applying the Lie derivative:

$$L^1 b^{1,1} = \sum_{i=1}^{3} b^{i,1} \frac{\partial}{\partial Y^i}(\sigma S).$$

Since $b^{1,1} = \sigma S$,

$$L^1(\sigma S) = (\sigma S)\frac{\partial}{\partial S}(\sigma S) = \sigma^2 S.$$

Similarly,

$$L^2(\sigma S) = pS.$$

Using equation (3.4):

$$S_{n+1} = S_n + \mu S_n \Delta t + \sigma_n S_n \Delta W_1 + \sigma_n^2 S_n J_{(1,1)} + p S_n J_{(2,1)}.$$

Discretizing for σ_t
- Drift term:

$$a^2 = \alpha(\xi - \sigma).$$

- Diffusion terms:

$$b^{2,1} = 0, \quad b^{2,2} = p.$$

Since $b^{2,2} = p$ is a constant,

$$L^1 b^{2,2} = 0, \quad L^2 b^{2,2} = 0.$$

So no correction terms appear.

$$\sigma_{n+1} = \sigma_n + \alpha(\xi_n - \sigma_n)\Delta t + p\Delta W_2.$$

Discretizing for ξ_t - Drift term:

$$a^3 = \beta(\sigma - \xi).$$

- Diffusion terms:

$$b^{3,1} = 0, \quad b^{3,2} = 0.$$

Since there are no stochastic terms in ξ_t, it remains a simple Euler step:

$$\xi_{n+1} = \xi_n + \beta(\sigma_n - \xi_n)\Delta t.$$

Final Milstein Scheme

$$S_{n+1} = S_n + \mu S_n \Delta t + \sigma_n S_n \Delta W_1 + \sigma_n^2 S_n J_{(1,1)} + p S_n J_{(2,1)},$$

$$\sigma_{n+1} = \sigma_n + \alpha(\xi_n - \sigma_n)\Delta t + p\Delta W_2,$$

$$\xi_{n+1} = \xi_n + \beta(\sigma_n - \xi_n)\Delta t.$$

where:

$$J_{(1,1)} \approx \frac{1}{2}\big[(\Delta W_1)^2 - \Delta t\big], \quad J_{(2,1)} \approx \Delta W_2 \Delta W_1.$$

If w_1 and w_2**are** correlated with correlation ρ, the Wiener increments must be generated as:

$$\Delta W_1 = \sqrt{\Delta t} Z_1, \quad \Delta W_2 = \rho\sqrt{\Delta t} Z_1 + \sqrt{1-\rho^2}\sqrt{\Delta t} Z_2,$$

where $Z_1, Z_2 \sim \mathcal{N}(0,1)$ are independent standard normal variables.

3 Parameter Analysis

In this section we will look at the effect of altering the parameters σ and α on both the Euler-Maruyama scheme and the Milstein scheme. We have chosen to look at combinations of the following parameter values.

$$\alpha = 0.02, 5, 20 \tag{8}$$

$$p = 0.25, 1.25, 2.25 \tag{9}$$

Every run seen below, is an average of 1000 runs per α, p combination. Moreover, dt is set as 0.001 and $T = t_{end} = 1$.

As we consider the following three-equation stochastic differential system:

$$dS_t = \mu S_t \, dt + \sigma_t S_t \, dW_t^{(1)}, \tag{10}$$

$$d\sigma_t = -(\sigma_t - \xi_t) \, dt + p\sigma_t \, dW_t^{(2)}, \tag{11}$$

$$d\xi_t = \frac{1}{\alpha}(\sigma_t - \xi_t) \, dt, \tag{12}$$

we theoretically expect the following behaviour:

1. The parameter p controls the magnitude of the random shocks in σ_t. Higher p leads to greater stochastic fluctuations in σ_t.

2. The parameter α dictates how quickly ξ_t reverts to σ_t. If α is large, then $1/\alpha$ is small, meaning ξ_t adjusts slowly to σ_t. Conversely, a smaller α implies faster adjustment of ξ_t to σ_t.

   Since σ_t appears multiplicatively in the SDE for S_t, any additional variability or trends in σ_t directly impact the stock price paths. We will first analyse the effects of paramter tuning onξ_t and σ_t before we move on to the stock price. We will briefly discuss impact of α, p and if there is any difference between the schemes.

3.1 Influence of α and p on σ

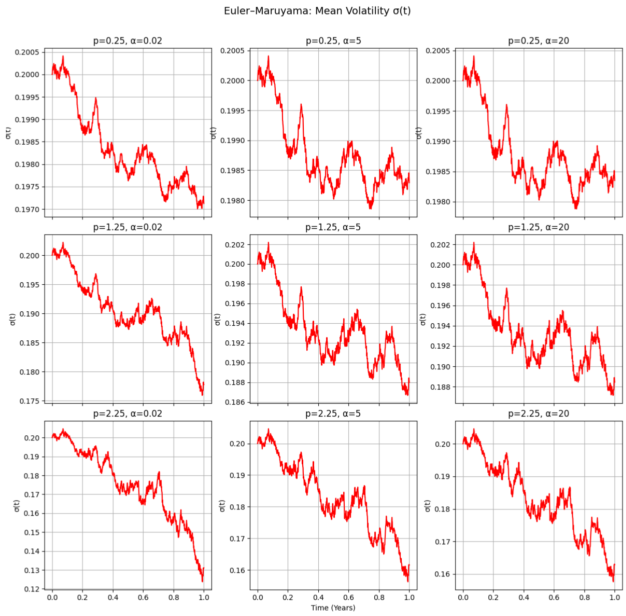

(a) Euler-Maruyama: Mean Volatility $\sigma(t)$

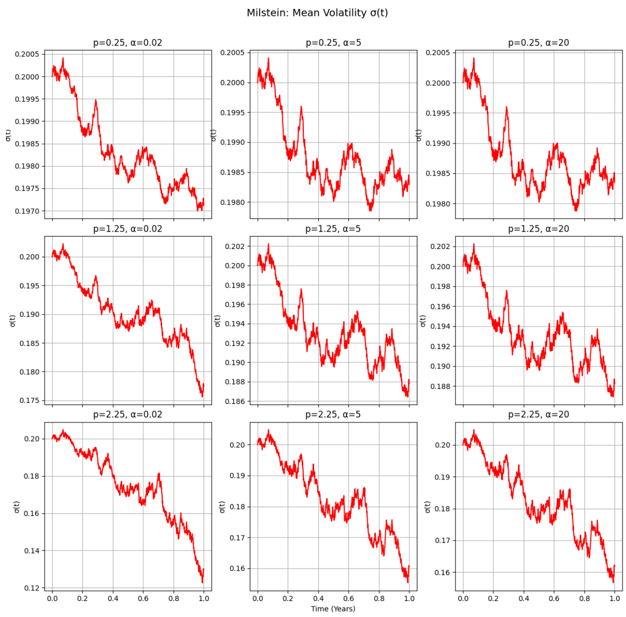

(b) Milstein: Mean Volatility $\sigma(t)$

Figure 1: Comparison of mean volatility using Euler-Maruyama and Milstein schemes

- **Influence of p.** The coefficient $p\sigma_t \, dw_t^{(2)}$ represents the noise term in the stochastic differential equation (SDE) for volatility. A larger p leads to stronger random fluctuations around the mean-reversion path. In time-series plots, this manifests as higher-frequency, higher-amplitude oscillations in $\sigma(t)$, visible as we move down the rows which corresponds to increasing p, as the values become more extreme as we go down comparing per column, i.e. regardless of alpha

- **Influence of α.** Although α does not explicitly appear in the SDE for σ_t, it determines the evolution of ξ_t, which influences the level to which σ_t is pulled. A larger α causes ξ_t to adjust more slowly, meaning that the "target" for σ_t remains near its initial value for a longer period before gradually decreasing. As a result, $\sigma(t)$ tends to decline more gradually in mean plots when α is large for this specific trajectory. This becomes visible comparing per row from left to right, with the graph on the left decreasing faster and therefore ending on more extreme values, regardless of p.

- **Euler vs. Milstein differences.** The qualitative dependence on p and α remains the same under both discretization schemes. However, Milstein's method provides slightly smoother or less-biased estimates of $\sigma(t)$ due to its correction term. Nevertheless, for sufficiently small time steps, both methods converge to the same limiting process.

3.2 Influence of α and p on ξ

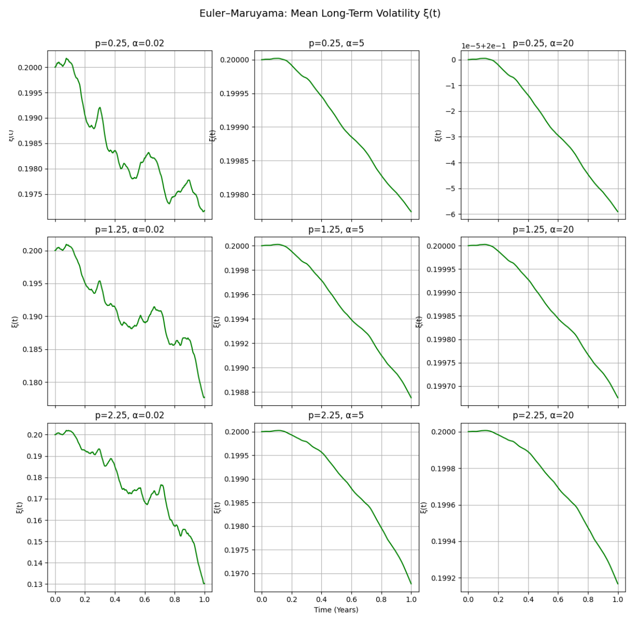

(a) Euler-Maruyama: Mean Long-Term Volatility $\xi(t)$

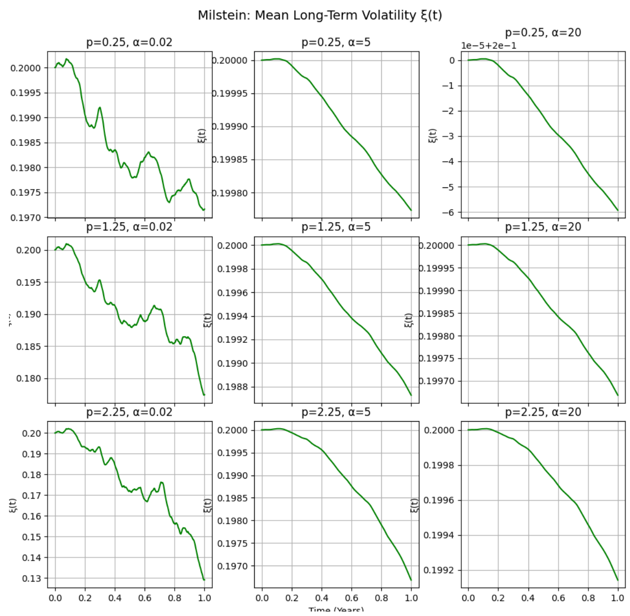

(b) Milstein: Mean Long-Term Volatility $\xi(t)$

Figure 2: Comparison of mean long-term volatility using Euler-Maruyama and Milstein schemes.

As time advances, ξ_t will move toward the level of σ_t.

For large α, since $\frac{1}{\alpha}$ is small, ξ_t is slow to adjust. This results in a gentle slope in the $\xi(t)$ plots, meaning that ξ_t remains near its initial level for a longer period and only gradually descends (or ascends) to match σ_t.

For smaller α, $\xi(t)$ "chases" $\sigma(t)$ more quickly; the curves exhibit more rapid adjustment.

This becomes mostly evident for the case with large p, where σ_t and we see that for small α, ξ follows quickly, and has stronger reactions to fluctuations in σ, whereas these phenomena become less expressed for larger values of α, visible if we move more to the right.

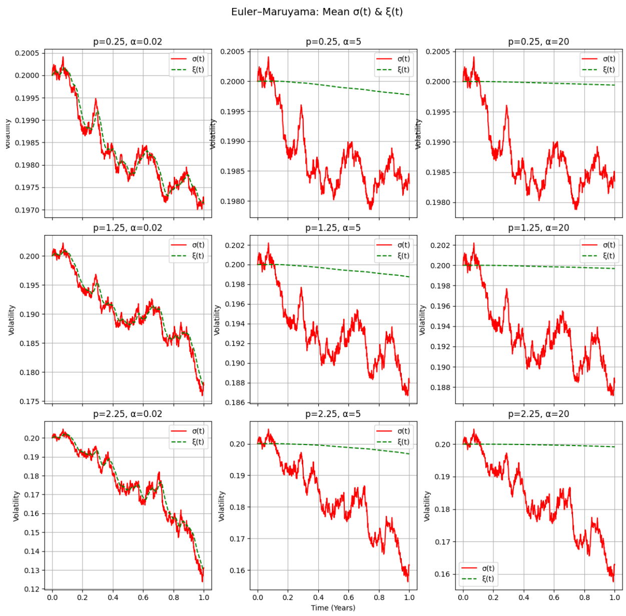

(a) Euler-Maruyama: Mean $\sigma(t)$ and $\xi(t)$

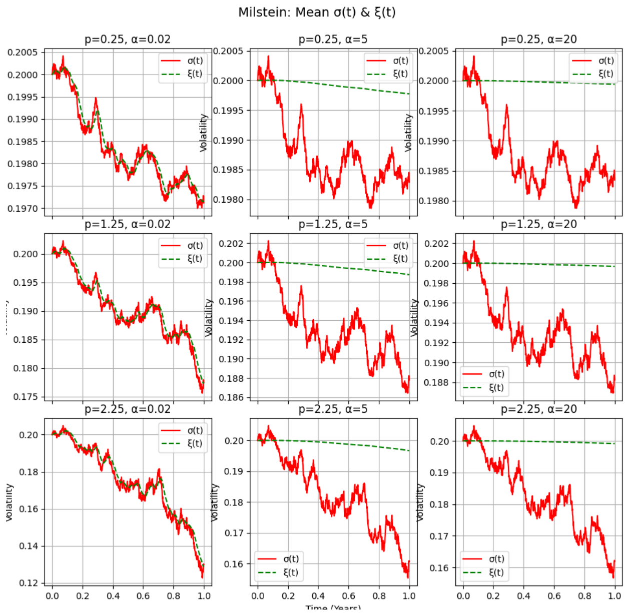

(b) Milstein: Mean $\sigma(t)$ and $\xi(t)$

Figure 3: Comparison of $\sigma(t)$ (red) and $\xi(t)$ (green, dashed) using Euler-Maruyama and Milstein schemes.

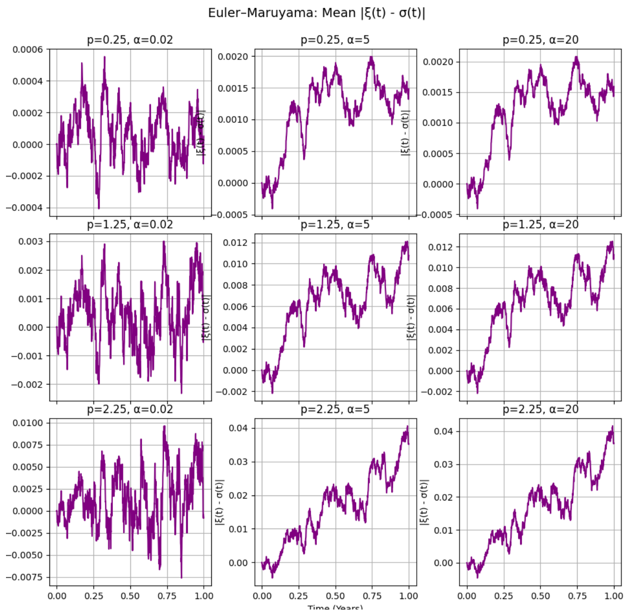

(a) Euler-Maruyama: Mean $|\xi(t) - \sigma(t)|$

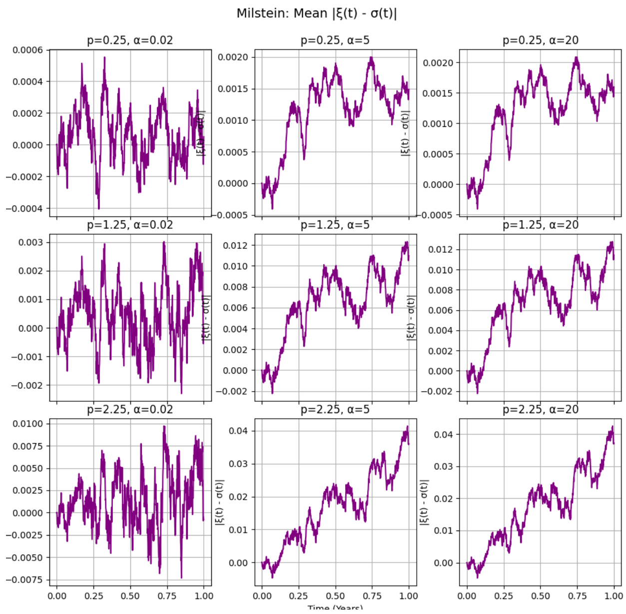

(b) Milstein: Mean $|\xi(t) - \sigma(t)|$

Figure 4: Comparison of mean absolute difference $|\xi(t) - \sigma(t)|$ using Euler-Maruyama and Milstein schemes.

The side-by-side plots of $\sigma(t)$ (red curves) and $\xi(t)$ (green dashed lines) illustrate how closely the instantaneous volatility σ_t tracks its long-run target ξ_t. When α is small, ξ_t quickly moves to wherever σ_t currently sits, keeping the two processes close—unless p is large, in which case σ_t can still jump quickly, leaving ξ_t struggling to keep up. When p is large, σ_t exhibits bigger stochastic swings, which can temporarily create larger gaps between $\sigma(t)$ and $\xi(t)$, even if α is small. These trends manifest as characteristic "wiggles" in σ_t around a gently sloping ξ_t.

The difference plots (purple-curve panels) illustrate the average absolute difference $|\xi(t) - \sigma(t)|$, highlighting when and by how much $\sigma(t)$ deviates from the long-term mean $\xi(t)$. Larger p generally increases this spread, as σ_t becomes more volatile, while larger α increases the early-time difference because ξ_t is slower to adjust. Conversely, when α is small, ξ_t rapidly tracks σ_t, reducing $|\xi(t)-\sigma(t)|$. Both Euler and Milstein discretizations exhibit the same patterns, with Milstein providing a somewhat smoother or less noisy estimate if the time step is not extremely small.

These trends manifest as the characteristic "wiggles" in σ_t around a gently sloping ξ_t in the plots.

3.3 Influence of α and p on Stock Price

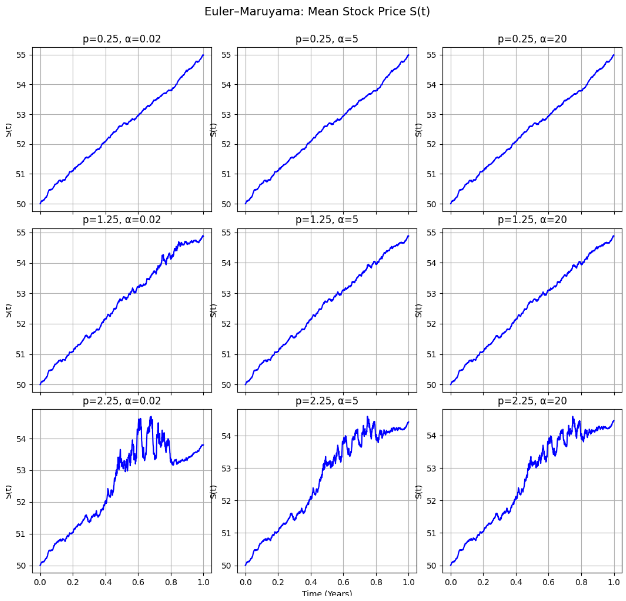

(a) Euler-Maruyama stock price

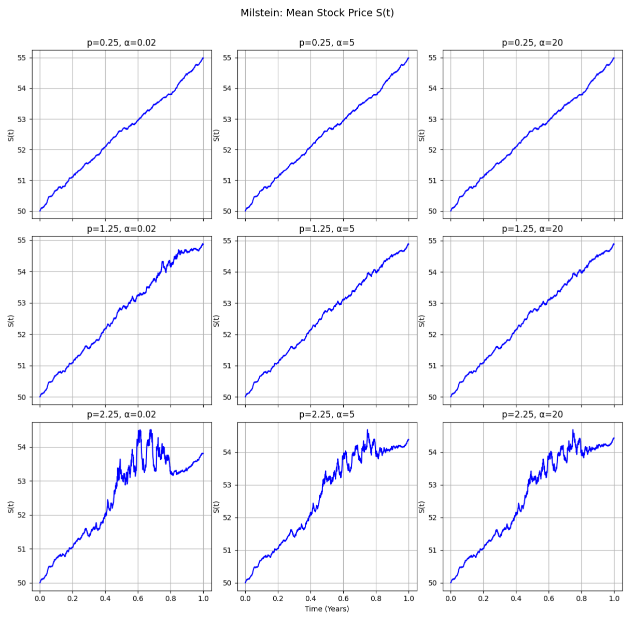

(b) Milstein stock price

Figure 5: Comparison of Euler-Maruyama and Milstein stock price simulations

The structure of the plots reveals the effects of the parameters p (volatility noise amplitude) and α (speed of mean reversion) on the dynamics of volatility σ_t, its long-run target ξ_t, and the resulting stock price $S(t)$. The insights from the individual volatility graphs (Sections 3–5) provide a deeper understanding of how these parameters interact.

Effect of p (Row-wise) Larger values of p increase the stochastic term in the volatility process, leading to more pronounced short-term fluctuations in $S(t)$, as seen in the red-curve volatility plots. When p is small (top row), σ_t remains relatively stable, producing smooth price trajectories that primarily follow the drift $\mu = 0.10$. As p increases (middle and bottom rows), σ_t exhibits greater variability, resulting in stronger short-term deviations in $S(t)$, consistent with the larger spreads observed in the difference plots $|\xi(t) - \sigma(t)|$.

Effect of α (Column-wise) The parameter α enters through the mean reversion equation:

$$d\xi_t = \frac{1}{\alpha}(\sigma_t - \xi_t)dt.$$

When α is small (left column), ξ_t quickly adjusts to match σ_t, leading to frequent mean-reversion episodes and more visible fluctuations in $S(t)$, aligning with the observations from the green-curve mean long-term volatility plots. When α is large (right column), ξ_t moves more gradually, stabilizing σ_t and leading to a smoother overall price trajectory. This effect is particularly pronounced for high-p settings, where slower adjustments in ξ_t prevent excessive short-term swings in $S(t)$, as seen in the combined plots of σ_t and ξ_t.

Euler–Maruyama vs. Milstein Both discretization schemes capture the same fundamental dynamics: mean reversion in σ_t and ξ_t, along with a multiplicative noise term. As seen in section 2, Milstein's correction term reduces discretization bias, yielding marginally more stable results. However, for this specific parameter set and short time horizon $[0, 1]$, the differences between the two methods are minimal, and both preserve the same parameter-driven effects.

Final Observations The interplay between p and α dictates both short-term volatility fluctuations and long-term persistence. As seen in the combined volatility plots, when p is small, σ_t remains close to a deterministic growth path, leading to a steady upward trend in $S(t)$. When p is large, short-term volatility increases, introducing greater stochastic variation. If α is small, ξ_t rapidly follows σ_t, making σ_t highly responsive to noise and causing $S(t)$ to exhibit more frequent fluctuations. Conversely, if α is large,

ξ_t adjusts slowly, leading to more prolonged deviations in σ_t and smoother long-term stock price evolution.

Ultimately, p governs the magnitude of short-term volatility swings, while α controls the timescale of mean reversion. Their combined effects shape the overall volatility profile of $S(t)$, determining whether the stock price exhibits high-frequency variability or a steadier long-term trend, as reflected across all volatility graph analyses.

4 Convergence Study

4.1 Strong Convergence for the Black-Scholes Model

In this section, we will look at the Black Scholes model,

$$dS_t = \mu S_t \, dt + \sigma_0 S_t \, dW_t, \quad S_0 > 0, \tag{13}$$

which has the well-known closed-form solution (for $0 \le t \le T$):

$$S_t = S_0 \exp\left((\mu - \frac{1}{2}\sigma_0^2)t + \sigma_0 W_t \right). \tag{14}$$

We compare the schemes' numerical solutions against the exact solution (under the same Brownian paths) and measure the strong error. The strong error for a single time T is measured for N Monte Carlo paths by:

$$\text{StrongError} = \left(\mathbb{E}\left[|S_T^{(\text{num})} - S_T^{(\text{exact})}|^2 \right] \right)^{1/2}, \tag{15}$$

where $S_T^{(\text{num})}$ is the approximation (Euler or Milstein) and $S_T^{(\text{exact})}$ is the true solution.

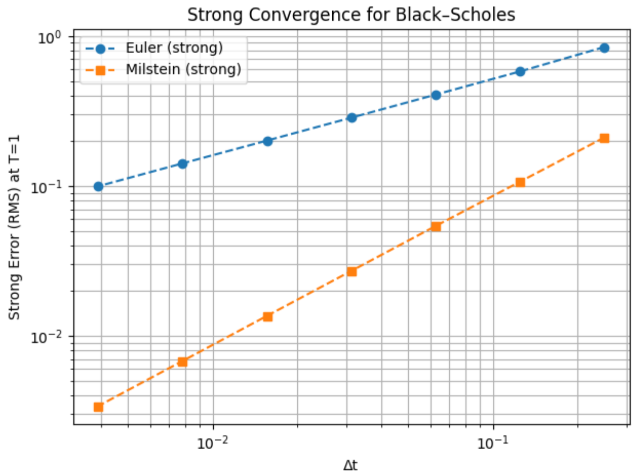

Figure 6: Strong Convergence for the Black-Scholes Model

In Figure 6 the RMS error at $T = 1$ can be seen for the Euler and Milstein scheme. Recall that the theoretical strong order of convergence is $\mathcal{O}(\sqrt{\Delta t})$ for the Euler scheme and $\mathcal{O}(\Delta t)$ for the Milstein scheme for scalar equations. Therefore, the Euler scheme is less accurate for small Δt. This can be seen in Figure 6 as the RMS error of the Milstein scheme is lower than that of the Euler scheme.

The slope of the RMS error for the Milstein scheme is approximately 1, corresponding tot the theoretical convergence rate of $\mathcal{O}(\Delta t)$. Similarly, the Euler scheme RMS error has a slope of approximately $\frac{1}{2}$, which also corresponds to the theoretical convergence of $\mathcal{O}(\sqrt{\Delta t})$.

Note that the slope of both error lines in the plot is different. The Euler scheme converges at a slower rate ($\mathcal{O}(\sqrt{\Delta t})$) than the Milstein scheme ($\mathcal{O}(\Delta t)$), due to the different order of convergence. The Milstein scheme shows a steeper decline in RMS error as Δt decreases, reflecting its faster convergence rate.

The higher-order term in the Milstein scheme reduces the truncation error, hereby significantly improving the accuracy. While the Milstein scheme is more accurate than the Euler scheme, it requires more computational resources than the Euler scheme.

4.2 Weak Convergence for the Black-Scholes Model

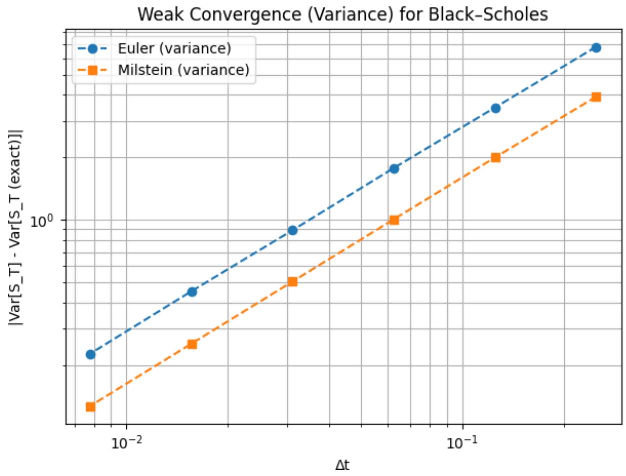

Figure 7: Weak Convergence for the Black-Scholes Model

Figure 7 shows the difference in variance of the stockprice between the simulated and exact solution. The theoretical weak order of convergence of both the Euler and Milstein scheme is $\mathcal{O}\Delta t$. This can be seen back in Figure 7 as the slope of both lines on the log-log plot is the same and is approximately 1.

The Milstein scheme has a better weak convergence than the Euler scheme, although both methods have the same weak order. The Milstein scheme includes a higher-order term which the Euler scheme does not. This can lower the weak error by reducing the bias. However, note that the Milstein scheme has a higher computational cost than the Euler method.

4.3 Full Model Analysis

Since the exact solution (S_t, σ_t, ξ_t) is not available in closed form, we produce a *reference* solution on a very fine grid (e.g. $\Delta t_{\text{fine}} = 1/2048$) using Milstein as it's order of convergence is better or equal to Euler, and treat the endpoint $(S_{\text{ref}}, \sigma_{\text{ref}}, \xi_{\text{ref}})$ at time $T = 1$ as "exact."

For the **strong convergence** test, we then choose a sequence of coarser step sizes Δt_k and re-simulate the paths using nested Brownian increments (i.e. summing blocks of fine-grid increments). We measure the L^2-error

$$\sqrt{\mathbb{E}\left[\left\|S^{(\text{coarse})} - S^{(\text{ref})}\right\|^2\right]}$$

and observe the expected order of convergence upon plotting against Δt_k on a log–log scale.

For the **weak convergence** test, we compare only the statistics (mean, variance) of the terminal S_T for both the coarse and the reference path. In particular, we compute

$$\left|\mathbb{E}[S_T^{(\mathrm{coarse})}] - \mathbb{E}[S_T^{(\mathrm{ref})}]\right| \quad \text{and} \quad \left|\mathrm{Var}[S_T^{(\mathrm{coarse})}] - \mathrm{Var}[S_T^{(\mathrm{ref})}]\right|.$$

Again we plot these errors versus Δt_k on a log–log scale and estimate the rate.

Our numerical results confirm the well-known fact that both Euler and Milstein schemes have *strong order* $\frac{1}{2}$ and 1, respectively, and *weak order* 1 for Euler and 1 for Milstein, though the constants differ.

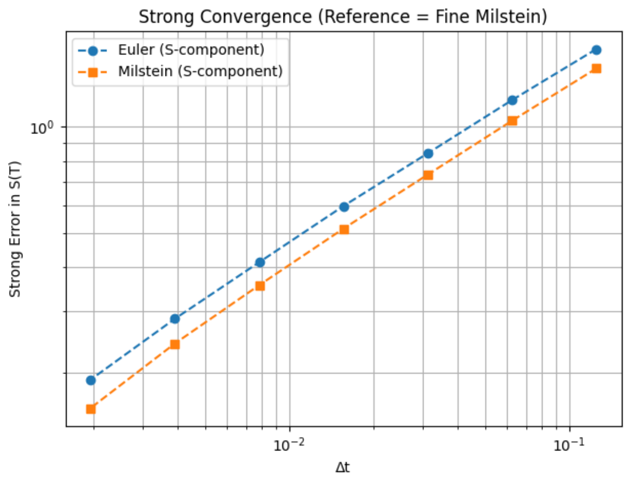

Figure 8: Strong Convergence for Full Model

Figure 8 contains the strong RMS error for the Euler and Milstein scheme. According to page 37 in the SDE notes on brightspace, for vector systems the order of convergence in the strong sense for a Milstein scheme is generally only $\mathcal{O}(\sqrt{\Delta t})$. The Euler scheme has the same order of convergence. This can be seen back in Figure 8 as both lines have the same slope of approximately $\frac{1}{2}$.

Moreover, note that the Milstein scheme has a slightly lower strong error than the Euler scheme. This is caused by the high-order correction term in the Milstein scheme, which reduces the truncation error.

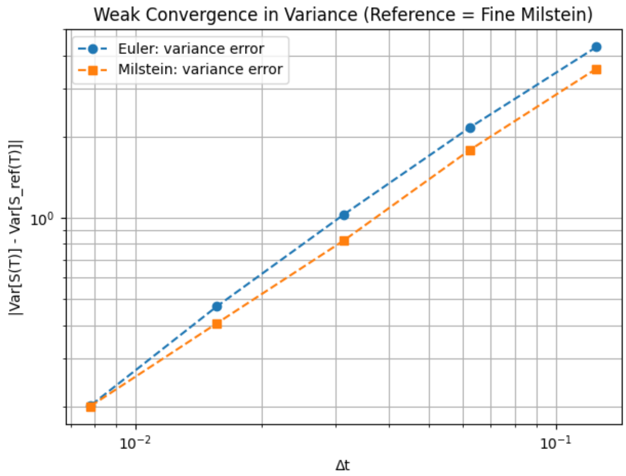

Figure 9: Weak convergence for full model

In Figure 9 the difference in variance of the stockprice of the simulation and reference (fine Milstein) can be found. Note that for larger Δt values, the Euler and Milstein scheme approximately have the same slope. The slope of both lines is approximately 1, corresponding to the theoretical order of convergence of $\mathcal{O}(\Delta t)$. They appear to converge to similar values as Δt gets smaller, but this is mostly due to noise. Running more paths should give a more accurate estimation of the weak error. However, we were unfortunately limited by the quality of the available CPU so this was not feasible.